Effect of the crossing-structure sequence on mixing performance within three-dimensional micromixers

Xiangsong Feng,[a)] Yukun Ren,[a),b)] and Hongyuan Jiang[b)]
School of Mechatronics Engineering, Harbin Institute of Technology, Harbin 150001, China

(Received 20 May 2014; accepted 21 May 2014; published online 2 June 2014)

The geometry of crossing structure formed by two-layer microchannels determines the axial and transverse movements of contact interface between two liquid streams, which gives us a new method for promoting the micromixers. Hence, we designed four different three-dimensional micromixers by selecting two different crossing structures as basic units (one unit is a crossing structure called "X" and the other is a reversed crossing structure called "rX"). In order to find out how the crossing-structure sequence affects the mixing performance within three-dimensional micromixers, we organized these four mixers in different ways, i.e., the first combination is X-rX-X-rX-…, the second is X-rX-rX-X-…, the third is X-X-rX-X-…, and the last one is X-X-X-X…. Consequently, quite distinct mixing phenomena are engendered. Furthermore, experiments were also conducted using the first and the last models to verify the simulation results. We infer that the last mixer is more likely to trigger chaos and convection by rotating the contact surface than the first one that merely swings the surface even when the flow rates and viscosities of the two liquid streams are increased. © *2014 AIP Publishing LLC*. [http://dx.doi.org/10.1063/1.4881275]

I. INTRODUCTION

In recent years, there has been an increasing interest in micromixers as an important component in microfluidic systems.[1,2] Mixing is an indispensable part in many microfluidic applications for chemical reactions,[3] protein crystallization,[4] biological assays,[5] and drug transfer.[6] In fact, it is difficult to mix small volumes of fluids in microfluidic system especially at low Reynolds number due to the laminar flows. To address this issue, many researchers always employ three-dimensional (3-D) channels,[7–9] staggered herringbone channels,[10,11] planar contraction/expansion channels,[12,13] curved channel with radial baffles,[14] or other ways[15–19] to efficiently mix dissimilar liquid streams.

Whitesides' group has devised a novel 3-D microstructure which can be used as an elastomeric microfluidic switch[20] and they find that the ratio of the height to the width of the channels strongly affects the flow pattern at the crossing region of the 3-D microchannel, thereby ensuring different switch functions. Interestingly, it can also lead to effective micromixing according to the exchange of fluid between the two crossing channels. In the last decade, many researchers have designed various 3-D micromixers with the crossing structure.[21–25] However, the study about the effect of the arrays of the crossings on the mixing performance is rarely explored.

In this paper, we proposed four 3-D models of micromixers in order to find the influence of crossing sequences on the mixing efficiency. At first, the micromixers were simulated and the flow patterns for these models were compared. In the following step, two of them are fabricated through multilayer soft lithography. The total length of the realized micromixers is 4.65 mm. Finally, the mixing experiments were accomplished to evaluate the performance

[a)]X. Feng and Y. Ren contributed equally to this work.
[b)]Authors to whom correspondence should be addressed. Electronic addresses: rykhit@hit.edu.cn and jhy_hit@hit.edu.cn.

quantitatively. These two micromixers exhibit rather different mixing performances over a wide Re range.

II. CHIP DESIGN AND NUMERICAL SIMULATIONS

To compare the effect of crossing-structure sequence on micromixing, we designed four different three-dimensional models by selecting two different crossing structures as basic units (one unit is the crossing structure called "X" structure and the other is the reversed crossing structure called "rX"). For the model in Fig. 1(a), the neighboring crossings are symmetrically connected like X-rX-X-rX-X-rX, so it is called as model XRX. For the model in Fig. 1(b), the neighboring crossings are connected like X-rX-rX-X-rX-rX, so it is called as model XRR. For the model in Fig. 1(c), the crossings are combined like X-X-rX-X-X-rX, so it is called as model XXR. For the model in Fig. 1(d), the crossings are repeatedly combined like X-X-X-X-X-X, so it is called as model XXX. All of these mixers are based on the concept of splitting and recombination. In model XRX, two branches of streams treated by one "X" unit flow directly into next "rX" unit. One cycle in model XRX consists of two units: "X" and "rX." In this way, one cycle in model XRR contains three units: "X," "rX," and "rX." And in model XXR, one cycle is also composed of three units: "X," "X," and "rX." In model XXX, one cycle only need one "X" structure. However, two liquid streams coming out from one "X" unit flow into next "X" unit in a different way in model XXX: the top fluid turns vertically into the bottom branch of next "X" and the bottom fluid is guided vertically into the top branch of next "X."

Structure wise, there is a common point that the two streams coming out from one "X" or "rX" structure are all reunited at the middle of next "X" or "rX" structure and then two treated liquid streams flow out. Note that this work is different from our previous work,[26] where the "H" and "O" structures between two neighboring "X" structures are totally different mixing

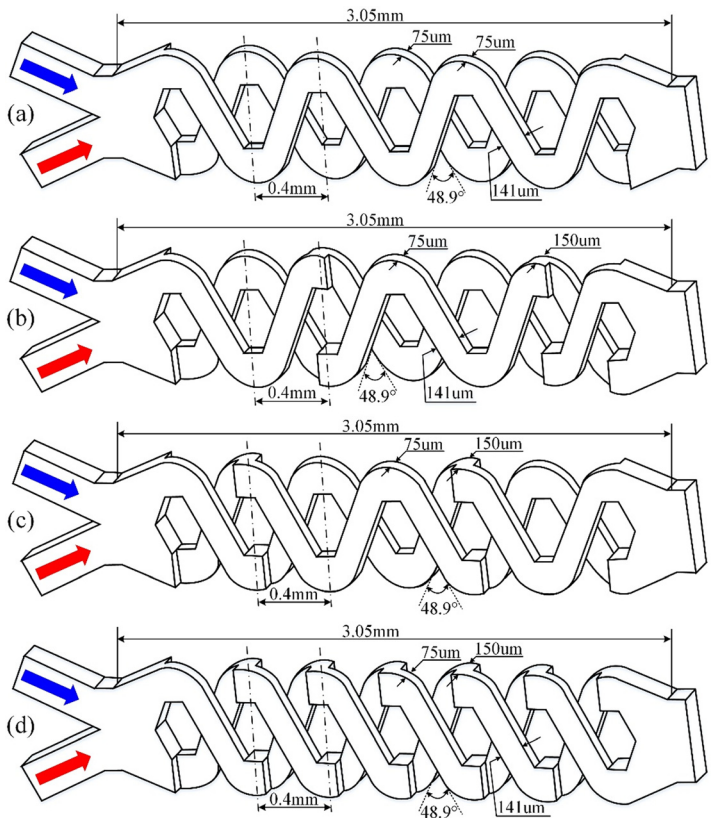

FIG. 1. Structures of the micromixers with six units and parameters involved. (a) Model XRX. (b) Model XRR. (c) Model XXR. (d) Model XXX.

units. Basically speaking, the "H" can recombine two liquid streams in the axial direction and the "O" directs two fluids with less contact. However, in this work, we focus on studying the effect of crossing-structure sequences on mixing with different motivations. The typical dimensions of the channel in each layer are 75 μm in depth and 141 μm in width, with a proper height-width ratio in order to accomplish near a half exchange between two liquid streams at the crossing area. Other relevant parameters are also shown in Fig. 1. More importantly, each crossing is formed by the top and bottom channels at a 48.9 angle, which not only shortens the total length of the micromixer but also enlarges the area of contact between the crossing channels compared with micromixer with tangential crossings. Therefore, we will obtain smarter and more effective mixing devices.

Two 2-layer polydimethylsiloxane (PDMS) devices for model XRX and XXX were fabricated according to our previous work.[26] We first make each PDMS layer with channels by using soft lithography. After treating the required sides of the top and bottom PDMS layers with oxygen plasma, we release a drop of deionized water for lubrication and then match and align the two parts using a "concave and convex" method[27] and bake dry at 60 °C for 3 h to bond. As shown in Fig. 2(a), these are the realized devices through the above process. Figs. 2(b) and 2(c) provide the images of the micromixers XRX and XXX, respectively, which were captured with the CCD camera.

Before performing the *in situ* experiment, numerical simulation was conducted to predict the mixing performance of the micromixers by commercial software COMSOL multiphysics (COMSOL 4.3, Sweden). In order to keep the simulation precision and save the computing time, tetrahedral grid systems were selected as the suitable grid systems for model XRX, model XRR, model XXR, and model XXX. And the corresponding element numbers are 7.6×10^5, 6.7×10^5, 6.5×10^5, and 6.3×10^5, respectively. In the simulation, the type of the fluid is incompressible Newton fluid governed by the Navier-Stokes equation, and the convective-diffusion equation is coupled with the flow field to simulate the transport of diluted species. And the flow was considered to be unaffected by gravity or centrifugal force, so these equations are represented as follows:

$$\nabla \cdot \vec{v} = 0, \tag{1}$$

$$\rho\left(\frac{\partial \vec{v}}{\partial t} + \vec{v} \cdot \nabla \vec{v}\right) = -\nabla p + \mu \nabla^2 \vec{v}, \tag{2}$$

$$\frac{\partial C}{\partial t} = D\nabla^2 C - \vec{v} \cdot \nabla C. \tag{3}$$

The flow is bounded by no-slip walls, ν is the flow velocity, C is the concentration of the solute, and the physical properties of water were utilized in the simulation (the density,

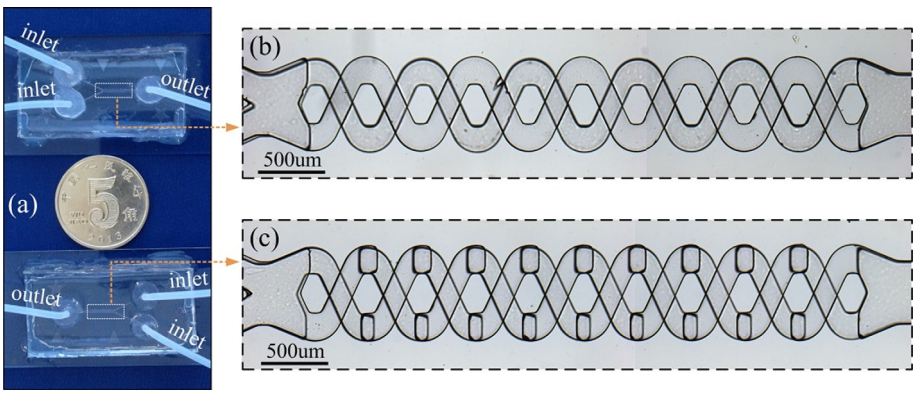

FIG. 2. Photographs of the XRX and XXX mixers. The scale bar is 500 μm. (a) The fabricated devices for models XRX and XXX. (b) Image of the micromixer XRX captured with the CCD camera. (c) Image of the micromixer XXX captured with the CCD camera.

$\rho = 997\,\text{kg/m}^3$, the dynamic viscosity, $\mu = 100$ cP, and the diffusion coefficient of the solute, $D = 1.0 \times 10^{-11}\ \text{m}^2/\text{s}$).

Fig. 3 compares the mixing characteristics in the first six units of model XRX, model XRR, model XXR, and model XXX at Re = 5.74. Note that different flow patterns are resulted from different arrays of the crossing structures. As shown in Fig. 3(a), the contact surface from the cross section at L = 0.625 mm to L = 2.625 mm in model XRX merely swings periodically from one side to another side. It is important to emphasize that there are two regions on both sides of the cross section at L = 2.625 where the concentration is near to $0\,\text{mol/m}^3$ on the left and $1\,\text{mol/m}^3$ on the right. Therefore, the fluids at both sides of the channel would not be fully mixed. As shown in Fig. 3(b), the interface from the cross section at L = 0.625 mm to L = 1.425 mm at first swings once and then rotates clockwise in one cycle of the model XRR. As shown in Fig. 3(c), the interface from the cross section at L = 0.625 mm to L = 1.425 mm at first rotates anticlockwise and then swings once in one cycle of the model XXR. Compared with model XRX, both model XRR and model XXR can rotate the contact surface because two neighboring units have the same crossing structure in one cycle (for instance, one "rX" is next to "rX" or "X" is next to "X"). And also there are some crossing units different from the front

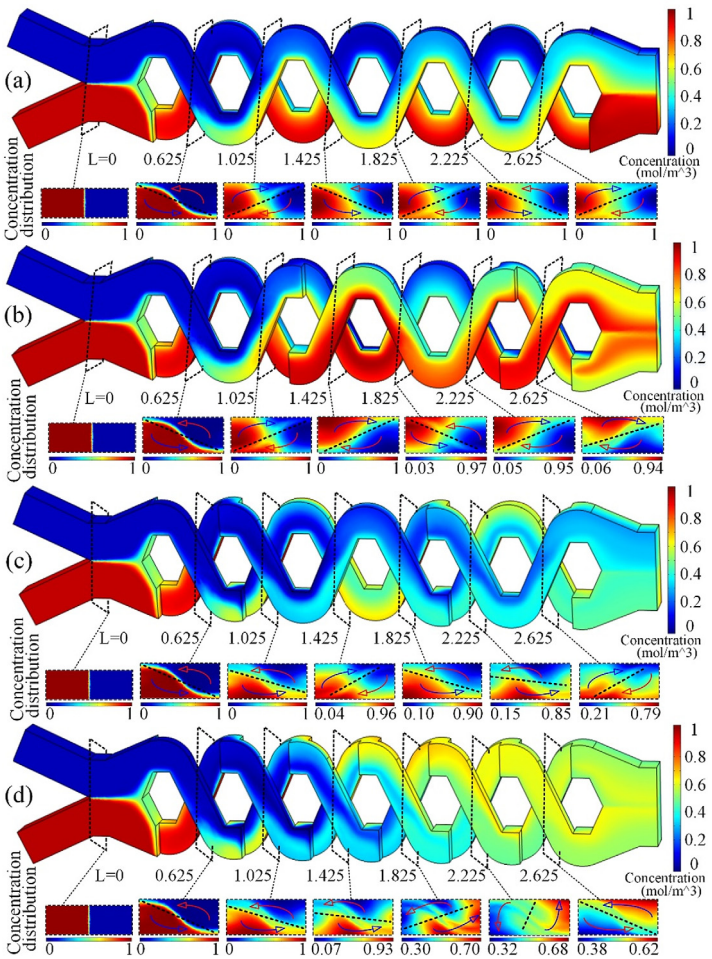

FIG. 3. Comparison of simulation results among model XRX, model XRR, model XXR, and model XXX. L indicates the mixer length. (a) Mixing of six units of model XRX and the distribution of concentration on the sampled planes, (b) mixing of six units of model XRR and the distribution of concentration on the sampled planes, (c) mixing of six units of model XXR and the distribution of concentration on the sampled planes, and (d) mixing of six units of model XXX and the distribution of concentration on the sampled planes. The sampled planes from L = 0.625 to L = 2.625 are at the middle of each "X" or reversed "X" structures. The concentrations of two dissimilar fluids to be mixed are $C = 0\,\text{mol/m}^3$ and $C = 1\,\text{mol/m}^3$ at the inlets.

units, which will prevent the rotating movement of the contact surface. So the mixing performance of model XRR and model XXR cannot be effectively enhanced. Therefore, we designed the fourth model XXX which is same to the model RRR. As shown in Fig. 3(d), the contact interface in model XXX always rotates anticlockwise. After six-unit mixing, the interface made a 180° rotation in the triangular transverse channel. Consequently, it is the continuous transverse rotation that enables the left/right fluid move to the right/left side. Obviously, the concentration on both sides of the cross section at L = 2.625 is near to 0.5 mol/m^3, which means that the fluids tend to be fully mixed. In essence, continuous transverse rotation is more prone to shorten the diffusion path and enhance the chaos and convection while the swinging flow pattern behaves worse. For this reason, we just employ model XRX and model XXX in the experiment to verify the effect of these two flow patterns on the mixing performance.

III. RESULTS AND DISCUSSION

Two groups of liquids with different viscosities are used to test the mixers. According to Lam's work,[28] we also want to know whether the flow pattern is changed under different viscosities. The first group includes: aqueous alkali with viscosity of 70 cP composed of 2.4 g sodium hydroxide (solute A), 30 g water, and 30 g glycerol and indicator with viscosity of 116 cP containing 1.5 g phenolphthalein (solute B), 30 g ethyl alcohol, and 30 g glycerol. The second group includes: aqueous alkali with viscosity of 380 cP composed of 1.2 g sodium hydroxide (solute A), 15 g water, and 60 g glycerol and indicator with viscosity of 393 cP containing 0.75 g phenolphthalein (solute B), 15 g ethyl alcohol, and 45 g glycerol. The aqueous alkali and the indicator were injected into the main channel from two inlets with same flow rates using a syringe pumps (LSP04-1A, China). After the streams meet, both the solutes will diffuse in the channel. Because the reaction between phenolphthalein and sodium hydroxide is very fast, we can neglect the time of the reaction. The color changes across the main channel were captured using a microscope (BX53, Olympus) equipped with a digital camera (Retiga-2000R). The color intensity from the captured images was analyzed using Image J (version 1.44p, USA).

Fig. 4 shows the mixing results of the straight channel (for control), mixer XRX and mixer XXX at Re = 5.74. For comparison, the straight channel as shown in Fig. 4(a) exhibits almost no chaotic convection. And the mixing only occurs in the middle of the straight channel. For mixer XRX in Fig. 4(b), there are three regions at the outlet of the mixer: unmixed aqueous alkali and indicator on both sides of the outlet and mixed solution in the middle. We find that it is difficult for the mixer XRX to mix the solutions on both sides of the channel, which has

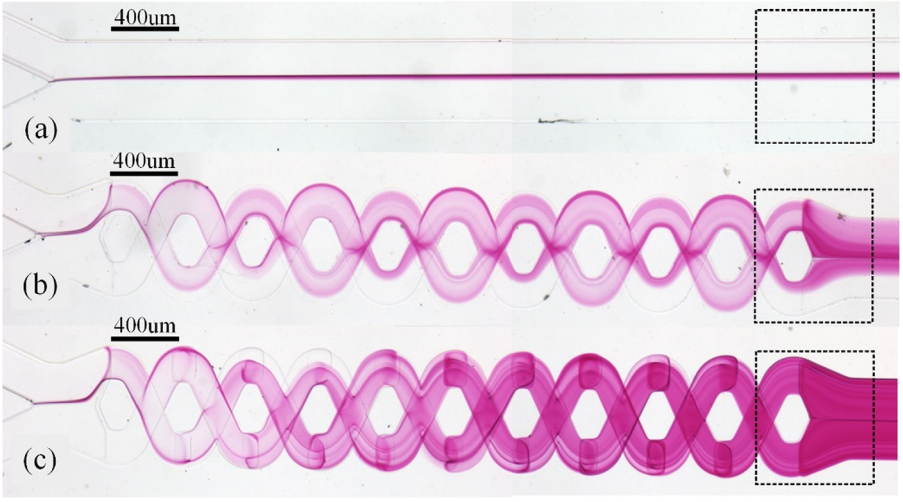

FIG. 4. Compare the experimental mixing results of these mixers at Re = 5.74. The scale bar is 400 μm. (a) The mixing result of the straight channel for comparison; (b) the mixing result of the mixer XRX at Re = 5.74; and (c) the mixing result of the mixer XXX Re = 5.74.

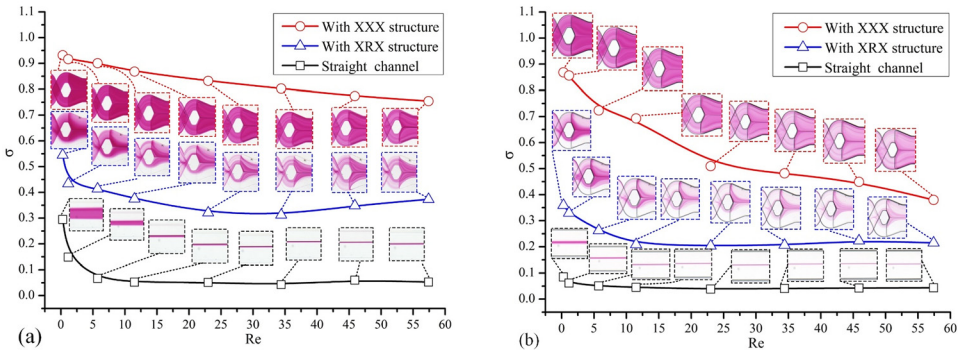

FIG. 5. Compare the mixing results at different Reynolds number of the mixers in experiment using two groups of viscous liquids. (a) Show the mixing efficiencies at the outlets of these mixers as a function of Re ranging from 0.3 to 57.4 when using the first group of liquids. (b) Show the mixing efficiencies at the outlets of these mixers as a function of Re ranging from 0.3 to 57.4 when using the second group of liquids.

good agreement with the simulation result as shown in Fig. 3(a). For mixer XXX in Fig. 4(c), the diffusion length is shortened and the mixed solution is uniformly distributed in whole channel of the outlet, which also could be expected from the simulation result as shown in Fig. 3(d).

In order to quantitatively compare the performance of mixer XRX and mixer XXX, we evaluate the mixing efficiencies $\sigma = 1 - \sqrt{(1/n)\sum (I_i - I_{min})^2/(I_{max} - I_{min})^2}$ at the outlets of these two mixers using two groups of viscous liquids at Re = 0.29, 1.15, 5.74, 11.5, 23, 34.4, 45.9, and 57.4 as shown in Fig. 5. In the equation, n, I_i, I_{max}, and I_{min} are the total number of pixels, the intensity at pixel i, the intensity at pixel i if no mixing or diffusion, and the intensity of the perfectly mixed solution at pixel i, respectively.

For the first group of liquids with low viscosity as shown in Fig. 5(a), when Re increases from 0.29 to 57.4, the efficiency reduces from about 93.2% to 75.4% for mixer XXX and the corresponding value declines from about 54.5% to 37.3% for mixer XRX. For the second group of liquids with high viscosity as shown in Fig. 5(b), when Re increases from 0.29 to 57.4, the efficiency reduces from about 86.8% to 38.0% for mixer XXX and the corresponding value declines from about 35.9% to 21.5% for mixer XRX. In this perspective, the mixer XXX is obviously more effective than mixer XRX. In Fig. 5, the images at the outlet of each mixer are attached under each Re number. From these images, we find that no matter Re number increases or the viscosities of the liquids used in experiments increase, each mixer keeps similar flow pattern. It is worth mentioning that mixer XXX could still make the left/right fluid move to the right/left side even when the viscosities of the liquids to be mixed increase to a high level.

IV. CONCLUSIONS

In conclusion, we have demonstrated four 3-D mixers with different arrays of crossing structures which generated obviously different motions of the contact interface, thereby showing different mixing performances. From the numerical and experimental results, we find that two dissimilar fluid streams with rotating contact surface are easier to be mixed than those with pendulum contact surface in rectangular channel even when we increase both the viscosities of the fluids and the Re number. It is because that continuous transverse rotation can obviously decrease the diffusion length and improve the chaos and convection.

ACKNOWLEDGMENTS

The authors wish to acknowledge China's Natural Science Foundation (Grant Nos. 51305106 and 11372093) and the Fundamental Research Funds for the Central Universities (Grant Nos. HIT. NSRIF. 2014058 and HIT. IBRSEM. 201319).

[1]P. Yager, T. Edwards, E. Fu, K. Helton, K. Nelson, M. R. Tam, and B. H. Weigl, Nature **442**, 412 (2006).
[2]Y. Wang, Q. Lin, and T. Mukherjee, Lab Chip **5**, 877 (2005).
[3]Y. Li, Y. Xu, X. Feng, and B.-F. Liu, Anal. Chem. **84**, 9025 (2012).
[4]C. L. Hansen, S. Classen, J. M. Berger, and S. R. Quake, J. Am. Chem. Soc. **128**, 3142 (2006).
[5]S. Li, Q. Yuan, B. I. Morshed, C. Ke, J. Wu, and H. Jiang, Biosens. Bioelectron. **41**, 649 (2013).
[6]J. Kim, Y. Jang, D. Byun, D. Hyung Kim, and M. Jun Kim, Appl. Phys. Lett. **103**, 103703 (2013).
[7]H. Chen and J.-C. Meiners, Appl. Phys. Lett. **84**, 2193 (2004).
[8]T. W. Lim, Y. Son, Y. J. Jeong, D.-Y. Yang, H.-J. Kong, K.-S. Lee, and D.-P. Kim, Lab Chip **11**, 100 (2011).
[9]H. Xia, Z. Wang, Y. Koh, and K. May, Lab Chip **10**, 1712 (2010).
[10]A. D. Stroock, S. K. Dertinger, A. Ajdari, I. Mezić, H. A. Stone, and G. M. Whitesides, Science **295**, 647 (2002).
[11]Y. Du, Z. Zhang, C. Yim, M. Lin, and X. Cao, Biomicrofluidics **4**, 024105 (2010).
[12]Y. Lam, H. Gan, N. Nguyen, and H. Lie, Biomicrofluidics **3**, 014106 (2009).
[13]M. G. Lee, S. Choi, and J.-K. Park, Appl. Phys. Lett. **95**, 051902 (2009).
[14]R.-T. Tsai and C.-Y. Wu, Biomicrofluidics **5**, 014103 (2011).
[15]M. Bengtsson and T. Laurell, Anal. Bioanal. Chem. **378**, 1716 (2004).
[16]H. Bockelmann, V. Heuveline, and D. P. Barz, Biomicrofluidics **6**, 024123 (2012).
[17]A. N. Hellman, K. R. Rau, H. H. Yoon, S. Bae, J. F. Palmer, K. S. Phillips, N. L. Allbritton, and V. Venugopalan, Anal. Chem. **79**, 4484 (2007).
[18]C. Y. Lim, Y. C. Lam, and C. Yang, Biomicrofluidics **4**, 014101 (2010).
[19]Z. Zhang, P. Zhao, G. Xiao, M. Lin, and X. Cao, Biomicrofluidics **2**, 014101 (2008).
[20]R. F. Ismagilov, D. Rosmarin, P. J. Kenis, D. T. Chiu, W. Zhang, H. A. Stone, and G. M. Whitesides, Anal. Chem. **73**, 4682 (2001).
[21]H. Xia, S. Wan, C. Shu, and Y. Chew, Lab Chip **5**, 748 (2005).
[22]L. Wang and J.-T. Yang, J. Micromech. Microeng. **16**, 2684 (2006).
[23]Y.-T. Chen, W.-F. Fang, Y.-C. Liu, and J.-T. Yang, Microfluid. Nanofluid. **11**, 339 (2011).
[24]D. Lee and Y. T. Chen, AIChE J. **57**, 571 (2011).
[25]D. Lee and P.-H. Lo, Chem. Eng. J. **181**, 524 (2012).
[26]X. Feng, Y. Ren, and H. Jiang, Biomicrofluidics **7**, 054121 (2013).
[27]A. Rotem, A. R. Abate, A. S. Utada, V. Van Steijn, and D. A. Weitz, Lab Chip **12**, 4263 (2012).
[28]H. Y. Gan, Y. C. Lam, and N.-T. Nguyen, Appl. Phys. Lett. **88**, 224103 (2006).